pubs.acs.org/journal/apchd5 Article

Realizing Tunable Evolution of Bound States in the Continuum and Circularly Polarized Points by Symmetry Breaking

Xinhao Wang,[§] Jiajun Wang,[*,§] Xingqi Zhao, Lei Shi,[*] and Jian Zi[*]

Cite This: https://doi.org/10.1021/acsphotonics.2c01522 Read Online

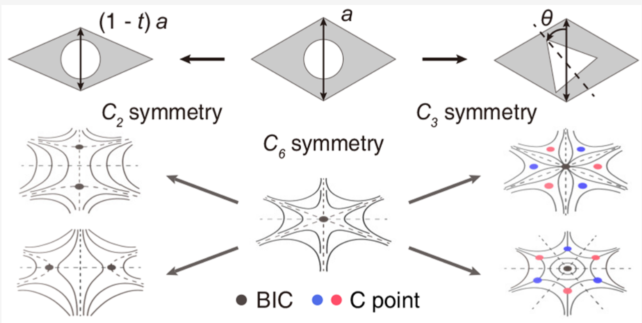

ABSTRACT: Bound states in the continuum (BICs) and circularly polarized points (C points), being well-known momentum-space polarization singularities in photonic crystal (PhC) slabs, have attracted much attention due to their novel properties. The further investigations on the generation and evolution of BICs and C points in momentum space have provided more perspectives to modulate these polarization singularities by tuning parameters. Recently, it was theoretically proposed that starting from a high-order BIC, various tunable evolutions of BICs and C points could be realized by symmetry breaking, offering an effective method to create and modulate polarization singularities in momentum space. To date, there is still no experimental realization of tunable evolution of polarization singularities from a high-order BIC. Here, we experimentally realized tunable evolution of BICs and C points in momentum space by symmetry breaking on purpose. The studied high-order BIC of −2 charge exists in a PhC slab of C_6 symmetry. The off-Γ BICs of −1 charge were observed by breaking the C_6 symmetry to the C_2 symmetry. The at-Γ BIC of +1 charge and off-Γ C points of $-\frac{1}{2}$ charge were observed by breaking the C_6 symmetry to the C_3 symmetry. The symmetry breaking factors and unit-cell configurations were further applied to continuously modulate the movement of polarization singularities in momentum space. Our results can promote the understanding of polarization singularities' evolution and provide effective approaches of symmetry breaking to on-purpose design BICs and C points in momentum space.

KEYWORDS: *photonic crystal slabs, momentum space, polarization singularities, bound states in the continuum, circularly polarized points*

■ INTRODUCTION

Momentum-space polarization singularities in photonic crystal (PhC) slabs have recently attracted much interest owing to their topological configurations and unique optical properties.[1−7] Being topological defects in momentum space, polarization singularities can carry polarization vortices with integer or half-integer winding numbers (topological charges), which topologically enable their exotic properties. The well-known examples of polarization singularities in PhC slabs are bound states in the continuum (BICs)[8−17] and circularly polarized points (C points).[18−21]

BICs are radiation singularities residing in the continuous leaky radiation spectra. Surrounding BICs, the states of polarization (SOPs) form vortices with integer topological charges,[9,11,12] which topologically enable infinite radiation lifetimes of BICs. Both the ultrahigh quality factors and the vortex configurations of BICs have been widely explored with various applications such as Bose−Einstein condensation,[22] lasing[23−25] and optical vortex generation,[26,27] nonlinear optics,[28−30] and so on.[31,32] Different from BICs, C points are leaky modes whose SOPs are circularly polarized. Around C points, SOPs form vortices with half-integer topological charges. Being closely related to the photon spin, C points have found applications in light−matter interactions and chiral emission,[33−35] among others.[36]

To promote the further applications, exploring effective approaches in controlling the momentum-space polarization singularities is of vital importance. The structure parameters, especially the symmetries, can be good degrees of freedom to manipulate the polarization singularities. It has been theoretically and experimentally observed that C points could spawn from the at-Γ BIC by breaking C_2 symmetry.[18] By breaking the up−down mirror symmetry, the unidirectional BIC was realized.[37,38] Recently, it was theoretically proposed that for the high-order polarization singularities, the symmetry breaking could lead to various evolution behaviors such as the

Special Issue: Photonics in China

Received: September 29, 2022

generation and annihilation of BICs and C points,[19] increasing modulation possibilities. The finding suggests a novel method by symmetry breaking to create and modulate various polarization singularities. However, up to now, the evolutions of high-order polarization singularities under symmetry breaking have not been experimentally realized.

In this work, we experimentally demonstrated the generation and the evolution of BICs and C points by breaking symmetry on purpose. A high-order BIC of −2 charge was observed in the PhC slab of triangular lattice with C_6 symmetry. By breaking the C_6 symmetry to the C_2 symmetry, two off-Γ BICs of −1 charge were split from the −2-charge BIC. By breaking the C_6 symmetry to the C_3 symmetry, one at-Γ BIC of +1 charge and six C points of $-\frac{1}{2}$ charge were generated from the −2-charge BIC. Furthermore, we demonstrated that BICs and C points can be manipulated in momentum space by tuning the symmetry-breaking factor and the unit-cell configuration.

RESULTS AND DISCUSSION

We start our discussions on a free-standing 2D PhC slab with C_6 symmetry, as shown in the left panel of Figure 1a. The slab

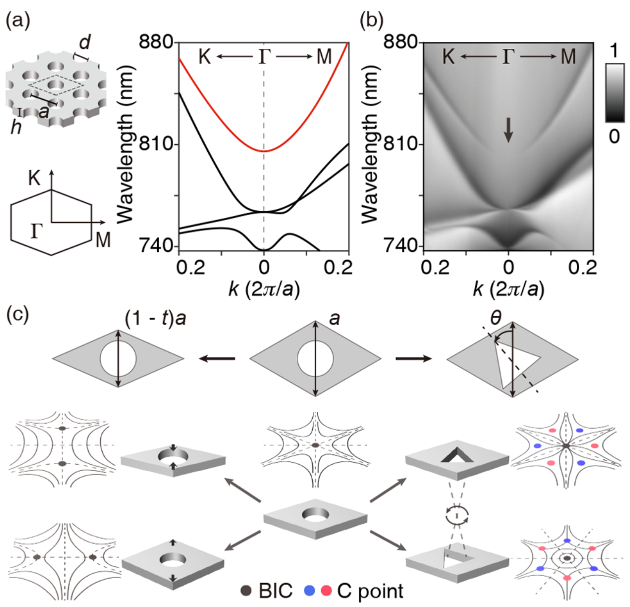

Figure 1. (a) Schematic view of the free-standing 2D PhC slab with a triangular lattice of circular air holes and the corresponding first Brillouin zone (left). Simulated TE-like band structure along the Γ-M and Γ-K directions (right). The band we focus on is marked by the red line. (b) The measured angle-resolved transmittance spectra under circularly polarized incidence. The vanished region marked by the black arrow is the at-Γ BIC with −2 charge. (c) Upper panel: schematic view of the unit cells of the PhC slabs with different in-plane symmetries: C_2 symmetry (left), C_6 symmetry (middle), and C_3 symmetry (right). Lower panel: illustration of the polarization vector fields in momentum space and their corresponding unit cells.

is made of silicon nitride (Si_3N_4, refractive index ∼2), of which the thickness h is 100 nm. Triangular lattices of circular air holes are etched on the slab, with period a = 724 nm and hole diameter d = 400 nm. The free-standing PhC slab maintains the up−down mirror symmetry because of the absence of the substrate, which makes the system simple and avoids extra diffractive channels.[39] In the right panel of the Figure 1a, by applying the finite element method, we calculated the TE-like band along the Γ-M and Γ-K directions. The band we focus on is marked by the red color, in which a symmetry-protected high-order BIC with −2 charge is at Γ point. The details of the polarization map and the quality factor distribution around the at-Γ BIC are exhibited in Sec. S1 of Supporting Information.

Starting from the symmetry-protected BIC, we could generate and manipulate various polarization singularities in momentum space under symmetry breaking and structural parameter tuning, as shown in Figure 1c. The polarization vector fields are presented in the form of streamlines which correspond to the connections of the main axes of the polarization states, from which we can clearly see the polarization singularities. The original at-Γ BIC with −2 charge is protected by the C_6 symmetry of the PhC slab;[9,11,19] thus, we can break the symmetry on purpose to control the further evolution of the high-order singularity from two perspectives: On the one hand, by breaking C_6 symmetry but preserving C_2 symmetry, the at-Γ BIC can be split into two off-Γ BICs with −1 charge. Compressing or stretching the unit cell would lead to different evolution trajectories of these off-Γ BICs. On the other hand, by breaking C_6 symmetry but preserving C_3 symmetry, the original BIC can be split into one at-Γ BIC with +1 charge and six C points with $-\frac{1}{2}$ charge. The existence of the at-Γ BIC is required by the C_3 symmetry.[9,11,19] Further, we can manipulate the rotation of C points in momentum space by rotating the etching holes in the unit cell while maintaining the C_3 symmetry. It is worth noting that all these processes are governed by the conservation of topological charges and structural symmetries.

To experimentally observe the evolution of high-order polarization singularities under symmetry breaking, we used electron beam lithography and the reactive-ion etching technique to fabricate the designed PhC slabs. Then we applied our homemade momentum space imaging spectroscopy system[11,40] to obtain the polarization-dependent angle-resolved transmittance spectra. The resonant process between the far-field incidence and the resonant modes of PhC slabs would lead to an obvious change of the transmittance, which can characterize the dispersion of photonic bands and corresponding SOPs. However, BICs cannot be excited by any far-field incidence, and C points cannot be excited by the far-field incidence with opposite circular polarizations. Hence, we can directly observe the evolution of polarization singularities in momentum space from nonexcited points of transmittance spectra of different polarizations.

Figure 1b shows the measured transmittance spectra along the Γ-M and Γ-K directions, which are in good agreement with the simulated band structure in Figure 1a. The vanished region marked by black arrow corresponds to the at-Γ BIC that cannot be excited by the far-field incidence. It is worth noting that the spectra are measured under circularly polarized incidence to obtain all the bands at one time. The details of the spectra under linearly polarized incidence are also shown in Sec. S2 of Supporting Information. We also measured the polarization-resolved iso-frequency contours to experimentally characterize the −2 charge of the at-Γ BIC (details are in Sec. S3 of Supporting Information).

To break C_6 symmetry but preserve C_2 symmetry, we can slight vary the longitudinal vector a while keeping the shape of the circular holes unchanged, shown as the left panel of Figure 1c. The symmetry-breaking parameter t is introduced to

https://doi.org/10.1021/acsphotonics.2c01522
ACS Photonics XXXX, XXX, XXX−XXX

describe the variation of the unit cells. For a positive (negative) t, the unit cell is compressed (stretched) relative to the original one ($t = 0$), resulting in the generation of off-Γ BICs along the Γ-Y (Γ-X) direction. As an example, we performed simulations for the cases of $t = \pm 0.06$, whose polarization maps and quality factor distributions are shown in Sec. S4 of Supporting Information. As our simulated results show, the SOPs are *s*-polarized along the Γ-X direction and *p*-polarized along the Γ-Y direction due to the mirror symmetry.

Then we experimentally fabricated PhC slabs with parameters $t = \pm 0.06$ and measured their transmittance spectra. Figure 2a,c show the *s*-polarized transmittance spectra

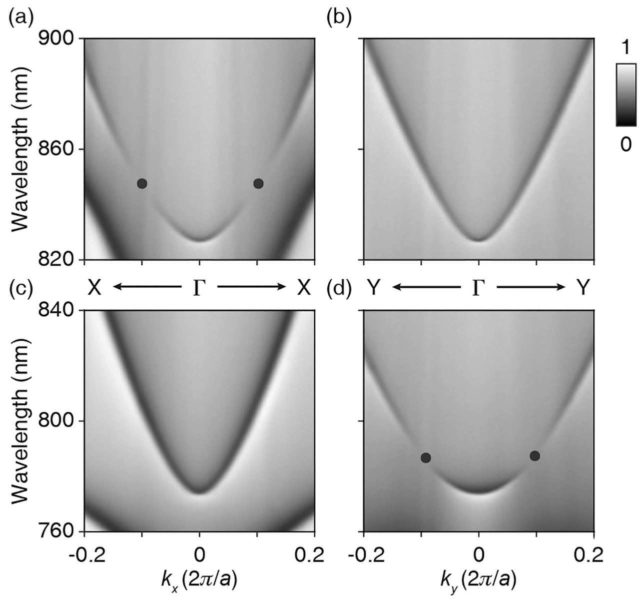

Figure 2. Measured angle-resolved transmittance spectra of the PhC slabs with C_2 symmetry. The black dots correspond to the off-Γ BICs. (a,b) The spectra of the $t = -0.06$ sample under *s*-polarized incidence (a) and *p*-polarized incidence (b). (c,d) The spectra of the $t = 0.06$ sample under *s*-polarized incidence (c) and under *p*-polarized incidence (d).

along the Γ-X direction, while Figure 2b,d show the *p*-polarized transmittance spectra along the Γ-Y direction. For the symmetry-broken PhC slab with $t = -0.06$, we can see there are a pair of vanished regions along the Γ-X direction (Figure 2a), in which the off-Γ BICs are marked by two dark dots. In contrast, for the symmetry-broken PhC slab with $t = 0.06$, a pair of vanished regions appear along the Γ-Y direction (Figure 2d). From the measured transmittance spectra, we directly observed the generated off-Γ BICs under symmetry breaking, and the results agree well with our simulations in the Supporting Information. The transmittance spectra measured under *p*-polarized incidence along the Γ-X direction and *s*-polarized incidence along the Γ-Y direction are also presented in Sec. S5 of Supporting Information.

Further, we show that we can continuously modulate the generated off-Γ BICs in momentum space by changing the parameter t. As exhibited in Figure 3, we prepared a series of samples with varying parameter t and measured their transmittance spectra. Figure 3a shows *s*-polarized transmittance spectra along the Γ-X direction for cases of $t < 0$. As t increases, the pair of off-Γ BICs move along the Γ-X direction and get closer to Γ point. When t is equal to 0, two off-Γ BICs merge into one at-Γ BIC. As t continues to increase ($t > 0$), the at-Γ BIC split into a pair of off-Γ BICs again and move farther away from Γ point along the Γ-Y direction (Figure 3b). In Figure 3c, we plot the momentum-space evolution trajectories of off-Γ BICs under the varying parameters t. The experimental results (black dots) are in good accordance with the simulated results (solid lines). These results proved the possibilities to purposefully control BICs in momentum space by symmetry breaking and provided a useful approach for us to generate and modulate the off-Γ BICs.

To break C_6 symmetry but preserve C_3 symmetry, we transformed the circular holes into regular triangular holes while keeping the shape of triangular lattice unchanged, as shown in the right panel of Figure 1c. The parameter θ is introduced to describe the rotational angle of the triangular holes. Note that the rotation of holes will not break C_3 symmetry. First, we take two C_3-symmetry PhC slabs with $\theta = 0°$ and 30° as examples, of which unit cells and the schematic view of polarization vector fields are shown in the right panel of Figure 1c. The detailed simulated polarization vector maps are shown in Sec. S6 of Supporting Information. The calculated results show that under this symmetry breaking, the at-Γ BIC with −2 charge is split into an at-Γ BIC with +1 charge and six off-Γ C points with $-\frac{1}{2}$ charge. For $\theta = 0°$ (30°), two C points are located at the Γ-M (Γ-K) direction, while along the Γ-K (Γ-M) direction, the SOPs are linearly polarized due to the mirror symmetry.

Figure 4a,b show the measured transmittance spectra of the fabricated PhC slabs. The spectra are measured under circularly polarized incidence to characterize the C points. First, we can see that in all measured spectra, there are unchanged vanished regions at Γ points marked by the black arrow. These vanished regions correspond to the at-Γ BIC protected by the C_3 symmetry. Second, there are regions which are vanished under some circularly polarized incidence while excited under the incidence with the opposite circular polarization, corresponding to the C points. Under the *RCP* (*LCP*) incidence, the red (blue) arrows mark the C points whose SOPs are *LCP* (*RCP*). In Figure 4a, for $\theta = 0°$, we can see that C points appear on the Γ-M axis. In contrast, for $\theta = 30°$, C points appear on the Γ-K axis (Figure 4b). From the measured spectra, the generation of polarization singularities under symmetry breaking from C_6 to C_3 symmetry has been directly observed and agrees well with the simulated results.

Further, we can continuously manipulate the rotation of the generated C points in momentum space by changing the parameter θ. To map the momentum-space evolution of C points with the varying θ from 0° to 30°, we first performed simulations to get polarization map of PhC slabs with different θ between 0° and 30° (details shown in the Supporting Information). We found that C points rotate in momentum space with the varying θ. Then we fabricated PhC slabs whose $\theta = 0°$, 10°, 20°, and 30° and measured their iso-frequency contours under circularly polarized incidences, as shown in Figure 4c. We selected a measurement wavelength of 846 nm with a bandpass filter (15 nm bandwidth), that is marked by the transparent stripe in Figure 4a. The results are obtained by $\frac{t_R - t_L}{t_R + t_L}$, where $t_L(t_R)$ corresponds to the transmittance under the *LCP* (*RCP*) incidence. The red (blue) color refers to regions whose SOPs are left-handed polarized (right-handed polarized), which can be used to characterize the location of C points. We can see that as θ varies from 0° to 30°, these

https://doi.org/10.1021/acsphotonics.2c01522
ACS Photonics XXXX, XXX, XXX−XXX

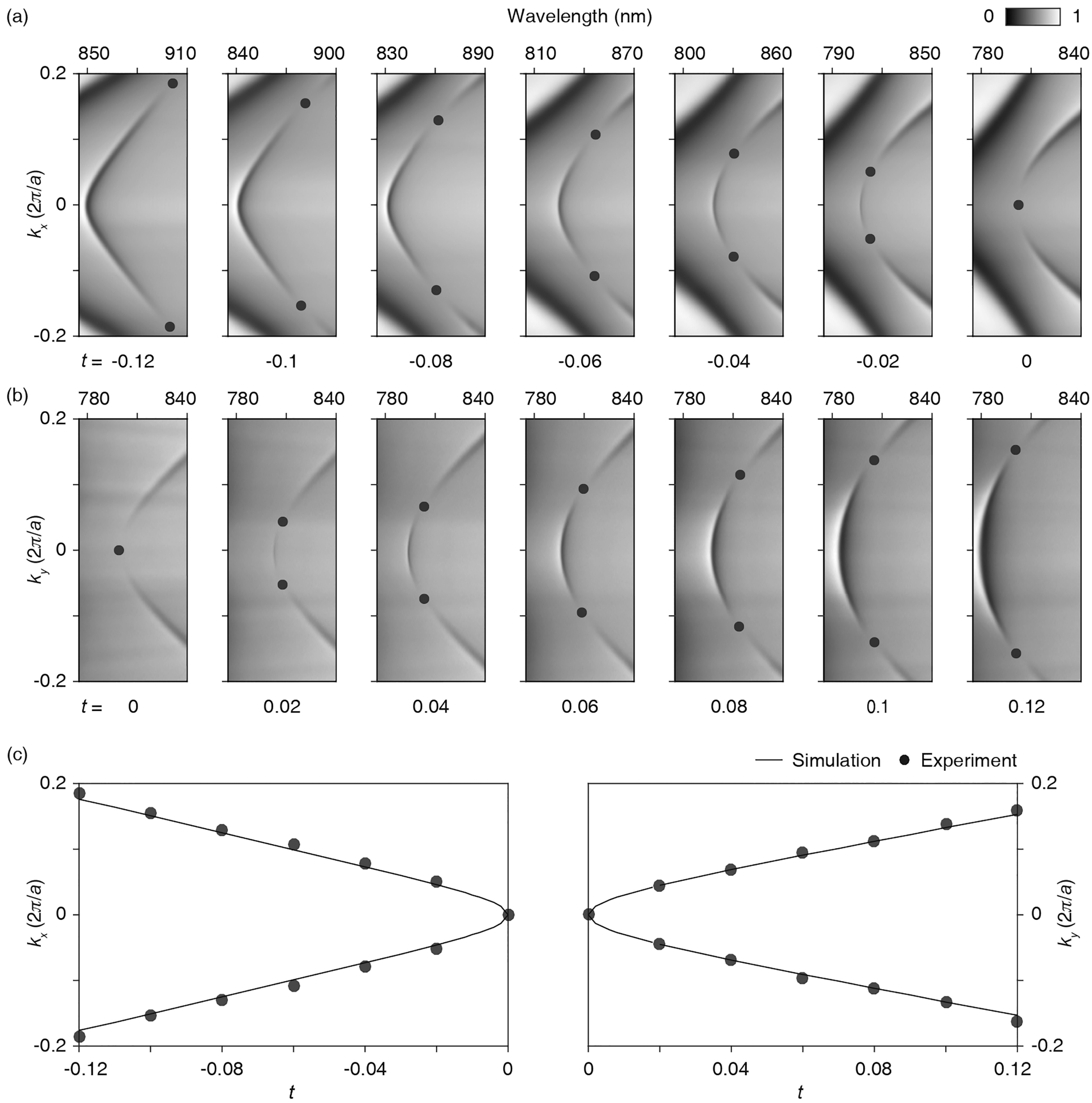

Figure 3. Evolutions of the off-Γ BICs in momentum space with the variation of parameter t. The black dots correspond to the BICs. (a,b) The measured angle-resolved transmittance spectra of the samples with different values of t. (a) The spectra along the Γ-X direction of the samples with "stretched" unit cells, s-polarized incidence. (b) The spectra along the Γ-Y direction of the samples with "compressed" unit cells, p-polarized incidence. (c) Trajectories of the BICs in momentum space as t varies.

colored regions with C points rotate in the same direction. The experimental results are in good agreement with simulated polarization maps. The results indicate that the structural parameters θ can also be a degree of freedom to manipulate rotation of C points in momentum space, offering us an effective approach to on purpose design the momentum polarization distribution with structural parameters of PhC slabs.

CONCLUSION

In conclusion, we have experimentally demonstrated various modulation schemes for polarization singularities by symmetry breaking and tuning the unit-cell configuration. Starting from the PhC slab of triangular lattice with C_6 symmetry, a high-order at-Γ BIC of −2 charge was experimentally observed and characterized. Off-Γ BICs were generated by breaking the C_6 symmetry to the C_2 symmetry and could be continuously modulated in momentum space by the symmetry-breaking factor. C points would spawn from the previous −2-charge at-Γ BIC by breaking the C_6 symmetry to the C_3 symmetry, and meanwhile another BIC of +1 charge emerged and was fixed at Γ point. These generated C points were rotated in momentum space by applying the rotation operation on the unit-cell configurations. The conservation of topological charges was kept in all these processes. We believe that, by giving experimental realizations of polarization singularities modulation, our work could offer effective approaches to purposefully designing BICs and C points in practical

https://doi.org/10.1021/acsphotonics.2c01522
ACS Photonics XXXX, XXX, XXX−XXX

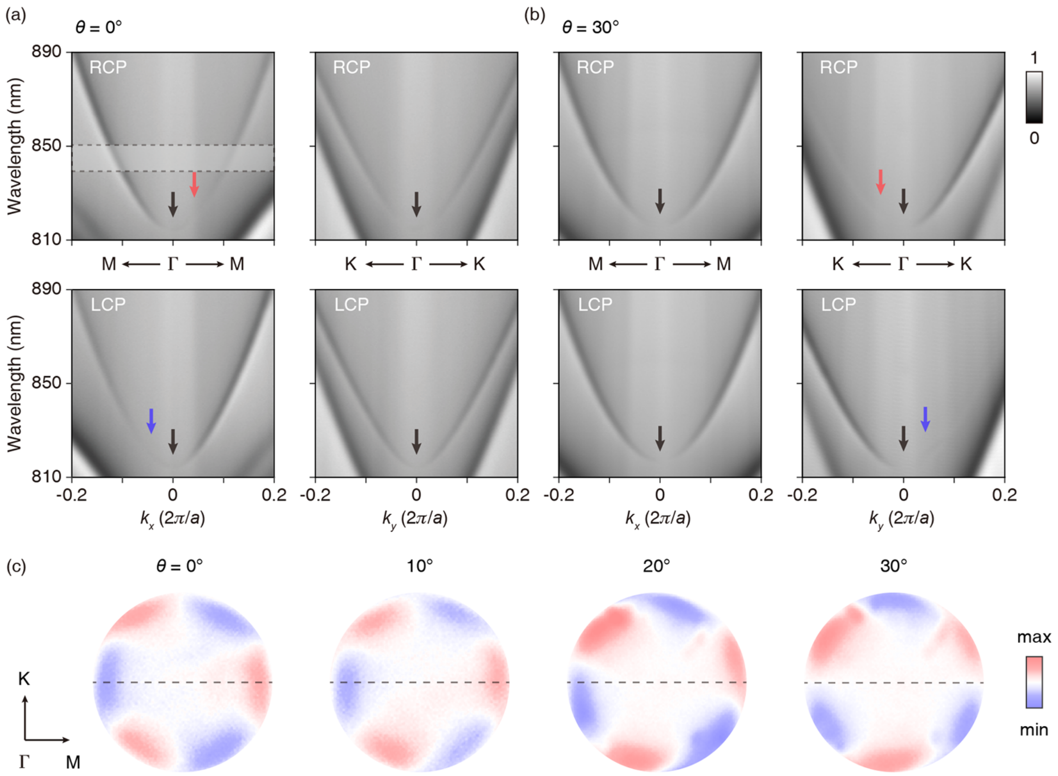

Figure 4. (a,b) The measured angle-resolved transmittance spectra of the PhC slabs with C_3 symmetry under right-handed circularly polarized (*RCP*) and left-handed circularly polarized (*LCP*) incidence. The vanished regions at the Γ point marked by black arrows are the at-Γ BICs with −1 charge. The vanished regions near the Γ point marked by red or blue arrows are *C* points. (a) The spectra of the $\theta = 0°$ sample. (b) The spectra of the $\theta = 30°$ sample. (c) The measured polarization-resolved iso-frequency contours of the C_3-symmetry PhC slabs with different values of θ at a central wavelength of 846 nm. The SOPs in red (blue) regions are left-handed polarized (right-handed polarized).

applications and pave the way for experimental investigations on polarization singularities evolutions.

■ ASSOCIATED CONTENT

Supporting Information

The Supporting Information is available free of charge at https://pubs.acs.org/doi/10.1021/acsphotonics.2c01522.

Calculated polarization map and quality factor distribution of PhC slab with C_6 symmetry, measured transmittance spectra of PhC slab with C_6 symmetry under linearly polarized incidence, measured polarization-resolved iso-frequency contours of PhC slab with C_6 symmetry, calculated polarization maps and quality factor distributions of PhC slabs with C_2 symmetry, supplementary transmittance spectra of PhC slabs with C_2 symmetry, calculated polarization maps and quality factor distributions of PhC slabs with C_3 symmetry, distributions of singularities for structures without rotational symmetries, discussions of the measured transmittance spectra (PDF)

■ AUTHOR INFORMATION

Corresponding Authors

Jiajun Wang − *State Key Laboratory of Surface Physics, Key Laboratory of Micro- and Nano-Photonic Structures (Ministry of Education) and Department of Physics, Fudan University, Shanghai 200433, China;* orcid.org/0000-0002-7554-370X; Email: jjwang19@fudan.edu.cn

Lei Shi − *State Key Laboratory of Surface Physics, Key Laboratory of Micro- and Nano-Photonic Structures (Ministry of Education) and Department of Physics, Fudan University, Shanghai 200433, China; Institute for Nanolectronic Devices and Quantum Computing, Fudan University, Shanghai 200433, China; Collaborative Innovation Center of Advanced Microstructures, Nanjing University, Nanjing 210093, China;* orcid.org/0000-0001-8458-3941; Email: lshi@fudan.edu.cn

Jian Zi − *State Key Laboratory of Surface Physics, Key Laboratory of Micro- and Nano-Photonic Structures (Ministry of Education) and Department of Physics, Fudan University, Shanghai 200433, China; Institute for Nanolectronic Devices and Quantum Computing, Fudan University, Shanghai 200433, China; Collaborative Innovation Center of Advanced Microstructures, Nanjing University, Nanjing 210093, China;* Email: jzi@fudan.edu.cn

Authors

Xinhao Wang − *State Key Laboratory of Surface Physics, Key Laboratory of Micro- and Nano-Photonic Structures (Ministry of Education) and Department of Physics, Fudan University, Shanghai 200433, China*

Xingqi Zhao − *State Key Laboratory of Surface Physics, Key Laboratory of Micro- and Nano-Photonic Structures (Ministry of Education) and Department of Physics, Fudan University, Shanghai 200433, China*

Complete contact information is available at:

https://doi.org/10.1021/acsphotonics.2c01522
ACS Photonics XXXX, XXX, XXX−XXX

https://pubs.acs.org/10.1021/acsphotonics.2c01522

Author Contributions

§X.W. and J.W. contributed equally to this work.

Notes

The authors declare no competing financial interest.

■ ACKNOWLEDGMENTS

The work was supported by the China National Key Basic Research Program 2022YFA1404800 and National Science Foundation of China (12234007 and 12221004). L.S. was further supported by Science and Technology Commission of Shanghai Municipality (19XD1434600, 2019SHZDZX01, 19DZ2253000, 20501110500, and 21DZ1101500).

■ REFERENCES

(1) Hsu, C. W.; Zhen, B.; Stone, A. D.; Joannopoulos, J. D.; Soljačić, M. Bound states in the continuum. *Nature Reviews Materials* **2016**, *1*, 16048.

(2) Koshelev, K.; Bogdanov, A.; Kivshar, Y. Meta-optics and bound states in the continuum. *Science Bulletin* **2019**, *64*, 836−842.

(3) Chen, W.; Chen, Y.; Liu, W. Singularities and poincaré indices of electromagnetic multipoles. *Physical review letters* **2019**, *122*, 153907.

(4) Sadrieva, Z.; Frizyuk, K.; Petrov, M.; Kivshar, Y.; Bogdanov, A. Multipolar origin of bound states in the continuum. *Phys. Rev. B* **2019**, *100*, 115303.

(5) Chen, W.; Chen, Y.; Liu, W. Line singularities and Hopf indices of electromagnetic multipoles. *Laser & Photonics Reviews* **2020**, *14*, 2000049.

(6) Sadreev, A. F. Interference traps waves in an open system: bound states in the continuum. *Rep. Prog. Phys.* **2021**, *84*, 055901.

(7) Chen, W.; Yang, Q.; Chen, Y.; Liu, W. Extremize optical chiralities through polarization singularities. *Phys. Rev. Lett.* **2021**, *126*, 253901.

(8) Hsu, C. W.; Zhen, B.; Lee, J.; Chua, S.-L.; Johnson, S. G.; Joannopoulos, J. D.; Soljačić, M. Observation of trapped light within the radiation continuum. *Nature* **2013**, *499*, 188−191.

(9) Zhen, B.; Hsu, C. W.; Lu, L.; Stone, A. D.; Soljačić, M. Topological nature of optical bound states in the continuum. *Physical review letters* **2014**, *113*, 257401.

(10) Yang, Y.; Peng, C.; Liang, Y.; Li, Z.; Noda, S. Analytical perspective for bound states in the continuum in photonic crystal slabs. *Physical review letters* **2014**, *113*, 037401.

(11) Zhang, Y.; Chen, A.; Liu, W.; Hsu, C. W.; Wang, B.; Guan, F.; Liu, X.; Shi, L.; Lu, L.; Zi, J. Observation of polarization vortices in momentum space. *Physical review letters* **2018**, *120*, 186103.

(12) Doeleman, H. M.; Monticone, F.; den Hollander, W.; Alù, A.; Koenderink, A. F. Experimental observation of a polarization vortex at an optical bound state in the continuum. *Nat. Photonics* **2018**, *12*, 397−401.

(13) Minkov, M.; Williamson, I. A.; Xiao, M.; Fan, S. Zero-index bound states in the continuum. *Physical review letters* **2018**, *121*, 263901.

(14) Jin, J.; Yin, X.; Ni, L.; Soljačić, M.; Zhen, B.; Peng, C. Topologically enabled ultrahigh-Q guided resonances robust to out-of-plane scattering. *Nature* **2019**, *574*, 501−504.

(15) Kang, M.; Zhang, S.; Xiao, M.; Xu, H. Merging bound states in the continuum at off-high symmetry points. *Phys. Rev. Lett.* **2021**, *126*, 117402.

(16) Chen, Z.; Yin, X.; Jin, J.; Zheng, Z.; Zhang, Z.; Wang, F.; He, L.; Zhen, B.; Peng, C. Observation of miniaturized bound states in the continuum with ultra-high quality factors. *Science Bulletin* **2022**, *67*, 359−366.

(17) Kang, M.; Mao, L.; Zhang, S.; Xiao, M.; Xu, H.; Chan, C. T. Merging bound states in the continuum by harnessing higher-order topological charges. *Light: Science & Applications* **2022**, *11*, 228.

(18) Liu, W.; Wang, B.; Zhang, Y.; Wang, J.; Zhao, M.; Guan, F.; Liu, X.; Shi, L.; Zi, J. Circularly polarized states spawning from bound states in the continuum. *Phys. Rev. Lett.* **2019**, *123*, 116104.

(19) Yoda, T.; Notomi, M. Generation and annihilation of topologically protected bound states in the continuum and circularly polarized states by symmetry breaking. *Phys. Rev. Lett.* **2020**, *125*, 053902.

(20) Ye, W.; Gao, Y.; Liu, J. Singular points of polarizations in the momentum space of photonic crystal slabs. *Phys. Rev. Lett.* **2020**, *124*, 153904.

(21) Chen, W.; Yang, Q.; Chen, Y.; Liu, W. Evolution and global charge conservation for polarization singularities emerging from non-Hermitian degeneracies. *Proc. Natl. Acad. Sci. U. S. A.* **2021**, *118*, No. e2019578118.

(22) Ardizzone, V.; Riminucci, F.; Zanotti, S.; Gianfrate, A.; Efthymiou-Tsironi, M.; Suàrez-Forero, D.; Todisco, F.; De Giorgi, M.; Trypogeorgos, D.; Gigli, G.; et al. Polariton Bose−Einstein condensate from a bound state in the continuum. *Nature* **2022**, *605*, 447−452.

(23) Kodigala, A.; Lepetit, T.; Gu, Q.; Bahari, B.; Fainman, Y.; Kanté, B. Lasing action from photonic bound states in continuum. *Nature* **2017**, *541*, 196−199.

(24) Huang, C.; Zhang, C.; Xiao, S.; Wang, Y.; Fan, Y.; Liu, Y.; Zhang, N.; Qu, G.; Ji, H.; Han, J.; et al. Ultrafast control of vortex microlasers. *Science* **2020**, *367*, 1018−1021.

(25) Hwang, M.-S.; Lee, H.-C.; Kim, K.-H.; Jeong, K.-Y.; Kwon, S.-H.; Koshelev, K.; Kivshar, Y.; Park, H.-G. Ultralow-threshold laser using super-bound states in the continuum. *Nat. Commun.* **2021**, *12*, 4135.

(26) Wang, B.; Liu, W.; Zhao, M.; Wang, J.; Zhang, Y.; Chen, A.; Guan, F.; Liu, X.; Shi, L.; Zi, J. Generating optical vortex beams by momentum-space polarization vortices centred at bound states in the continuum. *Nat. Photonics* **2020**, *14*, 623−628.

(27) Liu, W.; Liu, W.; Shi, L.; Kivshar, Y. Topological polarization singularities in metaphotonics. *Nanophotonics* **2021**, *10*, 1469−1486.

(28) Carletti, L.; Koshelev, K.; De Angelis, C.; Kivshar, Y. Giant nonlinear response at the nanoscale driven by bound states in the continuum. *Physical review letters* **2018**, *121*, 033903.

(29) Liu, Z.; Xu, Y.; Lin, Y.; Xiang, J.; Feng, T.; Cao, Q.; Li, J.; Lan, S.; Liu, J. High-Q quasibound states in the continuum for nonlinear metasurfaces. *Physical review letters* **2019**, *123*, 253901.

(30) Liu, Z.; Wang, J.; Chen, B.; Wei, Y.; Liu, W.; Liu, J. Giant enhancement of continuous wave second harmonic generation from few-layer GaSe coupled to high-Q quasi bound states in the continuum. *Nano Lett.* **2021**, *21*, 7405−7410.

(31) Muhammad, N.; Chen, Y.; Qiu, C.-W.; Wang, G. P. Optical bound states in continuum in MoS2-based metasurface for directional light emission. *Nano Lett.* **2021**, *21*, 967−972.

(32) Dong, Z.; Jin, L.; Rezaei, S. D.; Wang, H.; Chen, Y.; Tjiptoharsono, F.; Ho, J.; Gorelik, S.; Ng, R. J. H.; Ruan, Q.; et al. Schrödinger's red pixel by quasi-bound-states-in-the-continuum. *Sci. Adv.* **2022**, *8*, No. eabm4512.

(33) Wang, J.; Li, H.; Ma, Y.; Zhao, M.; Liu, W.; Wang, B.; Wu, S.; Liu, X.; Shi, L.; Jiang, T.; et al. Routing valley exciton emission of a WS2 monolayer via delocalized Bloch modes of in-plane inversion-symmetry-broken photonic crystal slabs. *Light: Science & Applications* **2020**, *9*, 148.

(34) Zhang, X.; Liu, Y.; Han, J.; Kivshar, Y.; Song, Q. Chiral emission from resonant metasurfaces. *Science* **2022**, *377*, 1215−1218.

(35) Tian, J.; Adamo, G.; Liu, H.; Klein, M.; Han, S.; Liu, H.; Soci, C. Optical Rashba Effect in a Light-Emitting Perovskite Metasurface. *Adv. Mater.* **2022**, *34*, 2109157.

(36) Shi, T.; Deng, Z.-L.; Geng, G.; Zeng, X.; Zeng, Y.; Hu, G.; Overvig, A.; Li, J.; Qiu, C.-W.; Alù, A.; et al. Planar chiral metasurfaces with maximal and tunable chiroptical response driven by bound states in the continuum. *Nat. Commun.* **2022**, *13*, 4111.

(37) Yin, X.; Jin, J.; Soljačić, M.; Peng, C.; Zhen, B. Observation of topologically enabled unidirectional guided resonances. *Nature* **2020**, *580*, 467−471.

(38) Zeng, Y.; Hu, G.; Liu, K.; Tang, Z.; Qiu, C.-W. Dynamics of topological polarization singularity in momentum space. *Phys. Rev. Lett.* **2021**, *127*, 176101.
(39) Sadrieva, Z. F.; Sinev, I. S.; Koshelev, K. L.; Samusev, A.; Iorsh, I. V.; Takayama, O.; Malureanu, R.; Bogdanov, A. A.; Lavrinenko, A. V. Transition from optical bound states in the continuum to leaky resonances: role of substrate and roughness. *ACS Photonics* **2017**, *4*, 723−727.
(40) Zhang, Y.; Zhao, M.; Wang, J.; Liu, W.; Wang, B.; Hu, S.; Lu, G.; Chen, A.; Cui, J.; Zhang, W.; et al. Momentum-space imaging spectroscopy for the study of nanophotonic materials. *Science Bulletin* **2021**, *66*, 824−838.

https://doi.org/10.1021/acsphotonics.2c01522
ACS Photonics XXXX, XXX, XXX−XXX